Ruthenium Complexes of Six-Electron-Donor NUPHOS-Type Diphosphines: Highly Selective Catalysts for the Hydrocarboxylation of Terminal Alkynes

Simon Doherty,*,‡ Julian G. Knight,*,‡ Rakesh K. Rath,‡ William Clegg,‡ Ross W. Harrington,‡ Colin R. Newman,§ Robert Campbell,§ and Hiren Amin‡

School of Natural Sciences, Chemistry, Bedson Building, The University of Newcastle upon Tyne, Newcastle upon Tyne, NE1 7RU, U.K., and Centre for the Theory and Applications of Catalysis, School of Chemistry, The Queen's University of Belfast, David Keir Building, Stranmillis Road, Belfast, BT9 5AG, U.K.

Received January 6, 2005

The ruthenium-*p*-cymene complexes [(*p*-cymene)Ru(1,2,3,4-Me_4-NUPHOS)Cl][SbF_6] (**2a**) and [(*p*-cymene)Ru(1,4-Et_2-2,3-*cyclo*-C_6H_8-NUPHOS)Cl][SbF_6] (**2b**) have been prepared by reaction of [(*p*-cymene)$RuCl_2$]$_2$ with the corresponding NUPHOS diphosphine in the presence of $NaSbF_6$. The chloro ligand can be abstracted from these monocations to afford [(*p*-cymene)-Ru(*P*,*P*,η^2(*C*)-1,2,3,4-Me_4-NUPHOS)][SbF_6]$_2$ (**3a**) and [(*p*-cymene)Ru(*P*,*P*,η^2(*C*)-1,4-Et_2-2,3-*cyclo*-C_6H_8-NUPHOS)][SbF_6]$_2$ (**3b**), respectively, in which the diphosphine coordinates as a six-electron donor, bonded through both diphenylphosphino groups and one of the double bonds of the butadiene tether. In stark contrast, it proved markedly more difficult to abstract the chloro ligand from either the BIPHEP or the MeO-BIPHEP monocations [(*p*-cymene)-Ru(BIPHEP)Cl][SbF_6] (**4a**) and [(*p*-cymene)Ru(MeO-BIPHEP)Cl][SbF_6] (**4b**), and even after prolonged reaction times at elevated temperature [(*p*-cymene)Ru(BIPHEP)][SbF_6]$_2$ (**5a**) and [(*p*-cymene)Ru(MeO-BIPHEP)][SbF_6]$_2$ (**5b**) formed as a 30% mixture with unreacted **4a** and **4b**, respectively. The structures of **2a**, as its perchlorate salt, and **2b** have been determined by single-crystal X-ray crystallography and are compared with that of their BIPHEP counterpart **4a**. Unfortunately, it has not been possible to prepare the corresponding dppb complex [(*p*-cymene)Ru(dppb)Cl][SbF_6] to undertake a comparative study, since [(*p*-cymene)-$RuCl_2$]$_2$ reacts with dppb under the same conditions as those used to prepare **2a**,**b** to afford the bridged dimer [{(*p*-cymene)$RuCl_2$}$_2$(μ-dppb)] (**6**), the identity of which has been confirmed by a single-crystal X-ray study. Interestingly, **3a** undergoes rapid hydrolysis in the presence of pyridine to give [(*p*-cymene)Ru{Ph_2(O)PC(H)MeCMeCMeCMePPh_2}][SbF_6] (**7**), which contains an unusual unsymmetrical bisphosphine monoxide pincer ligand formed by oxidation of one of the diphenylphosphino groups of 1,2,3,4-Me_4-NUPHOS and a highly regioselective syn addition of Ru and H across the butadiene double bond proximate to the phosphine oxide. Dications **3a**,**b** catalyze the regioselective anti-Markovnikov addition of benzoic acid to 1-pentyne and 1-octyne to give the corresponding alk-1-en-1-yl esters with cis-to-trans ratios as high as 95:5, while the corresponding BIPHEP and MeO-BIPHEP complexes were significantly less selective, catalyst mixtures formed from **4b** giving a 70:30 mixture of cis and trans alk-1-en-1-yl ester. In contrast, selectivity was reversed with catalyst mixtures generated from **6**, which were 90% selective for Markovnikov addition to 1-octyne, as might have been predicted for a ruthenium catalyst coordinated by a single phosphine, albeit one-half of a bidentate diphosphine. Catalysts based on NUPHOS diphosphines are also highly active and selective for anti-Markovnikov addition of benzoic acid to phenylacetylene and give (*Z*)-styryl benzoate in yields of up to 85% and selectivities as high as 99:1 with no evidence for the formation of terminal olefin. In our hands, solutions formed by activation of **4a**,**b** with $AgSbF_6$ catalyze the regio- and stereoselective anti-Markovnikov hydrocarboxylation of phenylacetylene, which was somewhat surprising considering that an earlier report has claimed that **5b** reacts with phenylacetylene to form a stable catalytically inactive cyclometalation/insertion product.

Introduction

Biaryl-based diphosphines are proving to be among the most versatile and effective of ligands for asymmetric catalysis,[1] with noteworthy examples including the ruthenium-catalyzed asymmetric hydrogenation of

* To whom correspondence should be addressed. E-mail: s.doherty@ncl.ac.uk.
‡ The University of Newcastle upon Tyne.
§ The Queen's University of Belfast.

(1) (a) Seyden-Penne, J. *Chiral Auxiliaries and Ligands in Asymmetric Catalysis*: Wiley: New York, 1995. (b) Noyori, R. *Asymmetric Catalysis in Organic Synthesis*; Wiley: New York, 1994. (c) Ojima, I. Ed. *Catalytic Asymmetric Synthesis*, 2nd ed.; Wiley-VCH: New York, 2000.

10.1021/om050014j CCC: $30.25
Publication on Web 04/19/2005

olefins[2] and carbonyl compounds[3] as well as ring-opening polymerizations,[4] palladium-catalyzed transformations such as inter- and intramolecular Heck reactions,[5] hydroaminations (conjugate additions),[6] hydrocyanations,[7] Diels−Alder cycloadditions,[8] aldol and Mannich-type reactions,[9] and the ene reaction[10] and rhodium-catalyzed cycloisomerizations,[11] reductive aldol reactions,[12] kinetic resolutions,[13] and 1,6-additions to enynones.[14] Moreover, biaryl-based diphosphines have recently proven to be the ligand of choice for several achiral transformations, forming optimum catalysts for the carbonylation of heterocyclic chlorides,[15] the chemo- and regioselective intermolecular trimerization of alkynes,[16] Grignard cross-couplings,[17] and Buchwald−Hartwig aminations.[18]

We have recently prepared an entirely new class of diphosphine, NUPHOS, which is based on a 1,3-butadiene tether and a potential alternative to biaryl diphosphines such as BINAP and BIPHEP (Chart 1).[19] Preliminary studies have revealed that these diphosphines can coordinate as either 4e- or 6e-donors to ruthenium, with the third pair of electrons arising from

Chart 1

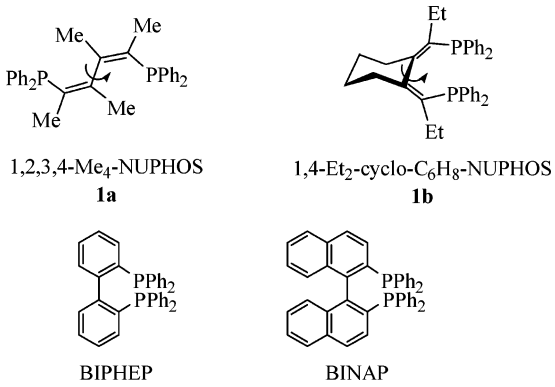

coordination of one of the carbon−carbon double bonds of the butadiene tether (eq 1).[20] Following this discovery, a survey of the literature revealed an increasing number of examples of biaryl diphosphines that coordinate in this manner, the first of which was reported by Pathak as early as 1994.[21] Pregosin subsequently prepared a number of related examples of six-electron-donor MeO-BIPHEP and BINAP ruthenium complexes, each supported by six-electron-donor hydrocarbons such as a deprotonated pyrrole, the benzene ring of indole, and *p*-cymene.[22] Biaryl diphosphines coordinated in this *P,P,*η^2(*C*)-manner are now routinely identified by a combination of ^{31}P and ^{13}C chemical shift data, the latter of which is obtained using long-range correlation.[23] In selected cases 2D NMR exchange spectroscopy has shown that the double bond is weakly coordinated and undergoes slow dissociative exchange.[22,23] More recently, James and co-workers have shown that [$RuCl_2$(BINAP)(bipy)] undergoes aerobic oxidation in methanol to give [RuCl(BINAPO)(bipy)][PF_6], which contains a six-electron (*P,O,*η^2-naphthyl) BINAP monoxide.[24]

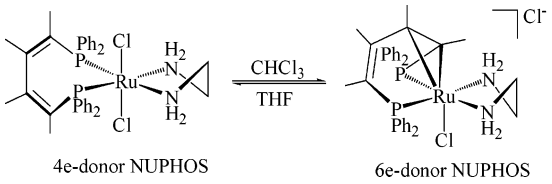

eq 1

Reasoning that the coordinated biaryl double bond of [(*p*-cymene)Ru(MeO-BIPHEP)][SbF_6]$_2$ could act to "stabilize" an otherwise coordinatively unsaturated 16-electron complex, this dication has been used to catalyze

(2) For a comprehensive and informative review see: (a) Noyori, R. *Angew. Chem., Int. Ed*. **2002**, *41*, 2008. See also: (b) Kitamura, M.; Tsukamoto, M.; Bessho, Y.; Yoshimura, M.; Kobs, U.; Widhalm, M.; Noyori, R. *J. Am. Chem. Soc*. **2002**, *124*, 6649. (b) Jeulin, S.; Duprat de Paule, S.; Ratovelomanana-Vidal, V.; Genet, J.-P.; Champion, N.; Dellis, P, *Proc. Nat. Acad. Sci*. **2004**, *101*, 5799. (c) Kitamura, M.; Kasahara, I.; Manabe, K.; Noyori, R.; Takaya, H. *J. Org. Chem*. **1988**, *53*, 708. (d) Noyori, R.; Ikeda, T.; Ohkuma, T.; Widhalm, M.; Kitamura, M.; Takaya, H.; Akutagawa, S.; Sayo, N.; Saito, T.; Taketomi, T.; Kumobayashi, H. *J. Am. Chem. Soc*. **1989**, *111*, 9134. (e) Noyori, R. *Tetrahedron* **1994**, *50*, 4259.

(3) (a) Noyori, R.; Ohkuma, *Angew. Chem., Int. Ed*. **2001**, *40*, 40. (b) Sandoval, C. A.; Ohkuma, T.; Muniz, K.; Noyori, R. *J. Am. Chem. Soc*. **2003**, *125*, 13490. (c) Qui, L.; Wu, J.; Chan, S.; Au-Yeung, T. T.-L.; Ji, J.-X.; Guo, R.; Pai, C.-C.; Zhou, Z.; Li, X.; Fan, Q.-H.; Chan, A. S. C. *Proc. Nat. Acad. Sci*. **2004**, *101*, 5815.

(4) Ameroso, D.; Fogg, D. E. *Macromolecule*s **2000**, *33*, 2815.

(5) (a) Ozawa, F.; Kubo, A.; Hayashi, T. *J. Am. Chem. Soc*. **1991**, *113*, 1417. (b) Ozawa, F.; Kubo, A.; Matsumoto, Y.; Hayashi, T.; Nishioka, E.; Yanagi, K.; Moriguchi, K. *Organometallics* **1993**, *12*, 4188.

(6) (a) Hii, K. K.; Li, K. *Chem. Commun*. **2003**, *1132*. (b) Li, K.; Cheng, X.; Hi, K. K. *Eur. J. Org. Chem*. **2004**, 959. (c) Hamashima, Y.; Somei, H.; Shimura, Y.; Tamura, T.; Sodeoka, M. *Org. Lett*. **2004**, *6*, 1861.

(7) Hodgson, M.; Parker, D. *J. Organomet. Chem*. **1987**, *325*, C27.

(8) (a) Ghosh, A. K.; Matsuda, H. *Org. Lett*. **1999**, *1*, 2157. (b) Oi, S.; Terada, E.; Ohuchi, K.; Kato, T.; Tachibana, Y.; Inoue, Y. *J. Org. Chem*. **1999**, *64*, 8660. (c) Hiroi, K.; Watanabe, K. *Tetrahedron: Asymmetry* **2001**, *12*, 3067. (d) Pignat, K.; Vallotto, J.; Pinna, F.; Strukul, G. *Organometallics* **2000**, *19*, 5160.

(9) (a) Sodeoka, M.; Tokunoh, R.; Miyazaki, F.; Hagiwara, E.; Shibasaki, M. *Synlett* **1997**, 464. (b) Fujimura, O. *J. Am. Chem. Soc*. **1998**, *120*, 10032. (c) Fujii, A.; Hagiwara, E.; Sodeoka, M. *J. Am. Chem. Soc*. **1999**, *121*, 5450.

(10) (a) Hao, J.; Hatano, M.; Mikami, K. *Org. Lett*. **2000**, *2*, 4059. (b) Aikawa, K.; Kainuma, S.; Hatano, M.; Mikami, K. *Tetrahedron Lett*. **2004**, *45*, 183. (c) Becker, J. J.; Van Orden, L. J.; White, P. S.; Gagné, M. R. *Org. Lett*. **2002**, *4*, 727. (d) Koh, J. H.; Larsen, A. O.; Gagné, M. R. *Org. Lett*. **2001**, *3*, 1233.

(11) (a) Lei, A.; Waldkirch, J. P. He, M.; Zhang, X. *Angew. Chem., Int. Ed*. **2002**, *41*, 4526. (b) Fairlamb, I. J. S. *Angew. Chem., Int. Ed*. **2004**, *43*, 1048. (c) Tong, X.; Dao, L.; Zhang, Z.; Zhang, X. *J. Am. Chem. Soc*. **2004**, *126*, 7601. (d) Mikami, K.; Yusa, Y.; Hatano, M.; Wakabayashi, K.; Aikawa, K. *Chem. Commun*. **2004**, 98.

(12) Morken, J. P.; Duffrey, M. O.; Taylor, S. J. *J. Am. Chem. Soc*. **2000**, *112*, 4528.

(13) (a) Tanaka, K.; Fu, G. C. *J. Am. Chem. Soc*. **2003**, *125*, 8078 (b) Tanaka, K.; Fu, G. C. *J. Am. Chem. Soc*. **2002**, *124*, 10296.

(14) Hayashi, T.; Tokunaga, N.; Inoue, K. *Org. Lett*. **2004**, *6*, 305.

(15) Albaneze-Walker, J.; Bazaral, C.; Leavey, T.; Dormes, P. G.; Murry, J. A. *Org. Lett*. **2004**, *6*, 2097.

(16) Tanaka, K.; Shirasaka, K. *Org. Lett*. **2003**, *5*, 4697.

(17) Ogasawara, M.; Yoshida, K.; Hayashi, T. *Organometallics* **2000**, *19*, 1567.

(18) (a) Wolfe, J. P.; Wagaw, S.; Marcoux, J.-F.; Buchwald, S. L. *Acc. Chem. Res*. **1998**, *31*, 805 (b) Hartwig, J. F. *Acc. Chem. Res*. **1998**, *31*, 852.

(19) (a) Doherty, S.; Knight. J. G.; Robins, E. G.; Scanlan, T. H.; Champkin, P. A.; Clegg, W. *J. Am. Chem. Soc*. **2001**, *123*, 5110. (b) Doherty, S.; Robins, E. G.; Nieuwenhuyzen, M.; Knight, J. G.; Champkin, P. A.; Clegg, W. *Organometallics* **2002**, *21*, 1383. (c) Doherty, S.; Newman, C. R.; Rath, R. K.; Hardacre, C.; Nieuwenhuyzen, M.; Knight, J. G. *Org. Lett.* **2003**, *5*, 3863. (d) Doherty, S.; Goodrich, P.; Hardacre, C.; Luo, H.-K.; Rooney, D. W.; Seddon, K. R.; Styring, P. *Green Chem*. **2004**, *6*, 63. (e) Doherty, S.; Newman, C. R.; Rath, R. K.; Hardacre, C.; Nieuwenhuyzen, M.; Knight, J. G. *Organometallics* **2004**, 23, 1055. (f) Doherty, S.; Knight, J. G.; Hardacre, C.; Luo, H.-K.; Newman, C. R.; Nieuwenhuyzen, M. *Organometallics* **2004**, *23*, 6127.

(20) Doherty, S.; Newman, C. R.; Hardacre, C.; Nieuwenhuyzen, M.; Knight, J. G. *Organometallics* **2003**, *22*, 1452.

(21) Pathak, D. D.; Adams, H.; Bailey, N. A.; King, P. J.; White, C. *J. Organomet. Chem*. **1994**, *479*, 237.

(22) Feiken, N.; Pregosin, P. S.; Trabesinger, G.; Albinati, A.; Evoli, G. L. *Organometallics* **1997**, *16*, 5756.

(23) (a) Feiken, N.; Pregosin, P. S.; Trabesinger, G.; Scalone, M. *Organometallics* **1997**, *16*, 537. (b) den Reijer, C. J.; Dotta, P.; Pregosin, P. S.; Albinati, A. *Can. J. Chem.* **2001**, *79*, 693.

(24) Cyr, P. W.; Rettig, S. J.; Patrick, B. O.; James, B. R. *Organometallics* **2002**, *21*, 4672.

Scheme 1

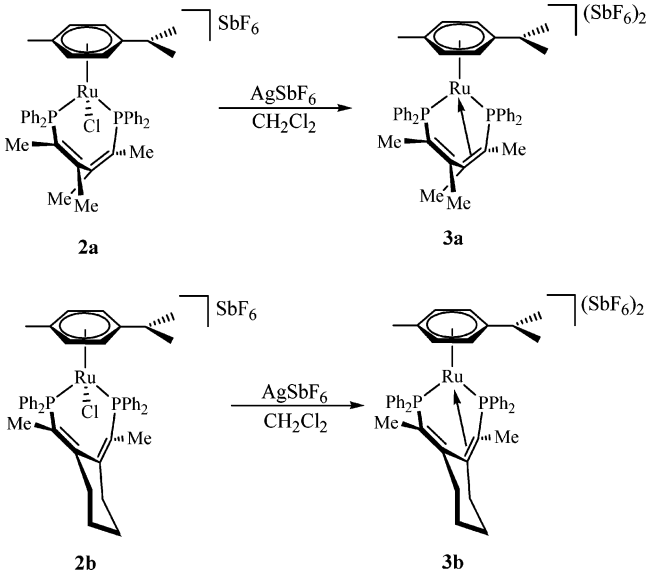

the anti-Markovnikov addition of benzoic acid to terminal alkynes.[25] While good cis/trans ratios were obtained for addition to 1-pentyne and 1-octyne, the dication was reported to be completely inactive for the reaction between phenylacetylene and benzoic acid, which was attributed to the formation of a stable, inactive cyclometalation-alkyne insertion product (vide infra). Herein, we report the results of a comparative study between the ruthenium-based chemistry of NUPHOS-type diphosphines and BIPHEP/MeO-BIPHEP, which has revealed several noteworthy differences including (i) a much greater propensity for NUPHOS diphosphines to coordinate in a *P*,*P*,η^2(*C*)-manner than BIPHEP or MeO-BIPHEP, (ii) markedly higher cis-to-trans ratios for anti-Markovnikov addition of benzoic acid to terminal alkynes with NUPHOS-based catalysts compared with their biaryl-based counterparts, and (iii) efficient and highly regio- and stereoselective addition of benzoic acid to phenylacetylene using catalysts based on NUPHOS.

Results and Discussion

Synthesis and Spectroscopic Characterization of Ruthenium(II) Complexes. Reaction of NUPHOS diphosphines **1a**,**b** with [(*p*-cymene)$RuCl_2$]$_2$ in dichloromethane in the presence of sodium hexafluoroantimonate gave salts of the monocations [(*p*-cymene)Ru(1,2,3,4-Me_4-NUPHOS)Cl][SbF_6] (**2a**) and [(*p*-cymene)Ru(1,4-Et_2-2,3-*cyclo*-C_6H_8-NUPHOS)Cl][SbF_6] (**2b**), respectively, in good yields (Scheme 1). Both complexes were isolated as orange-yellow solids after crystallization and were characterized by NMR spectroscopy, mass spectrometry, and elemental analysis. The ^{31}P NMR spectra of both **2a** and **2b** contain a pair of well-resolved doublets associated with the diastereotopic diphenylphosphino groups. The methyl region of the ^{1}H NMR spectrum of **2a** contains a set of four equal intensity signals associated with the four-carbon tether of NUPHOS, while that of **2b** is more complex due to the methylene protons of the cyclohexyl ring; both spectra contain a set of four well-resolved high-field-shifted doublets characteristic of the *p*-cymene ring. A similar procedure was used to prepare the corresponding BIPHEP and known MeO-BIPHEP complexes [(*p*-cymene)Ru(BIPHEP)Cl][SbF_6] (**4a**) and [(*p*-cymene)Ru(MeO-BIPHEP)Cl][SbF_6] (**4b**), respectively, again identified by a characteristic pair of doublets in the ^{31}P NMR spectrum. We also attempted to prepare the corresponding dppb complex [(*p*-cymene)Ru(dppb)Cl][SbF_6] to compare the performance of catalysts based on diphosphines containing a four-carbon sp^2-hydridized tether with that containing solely sp^3-hybridized carbon atoms. However, under the same conditions as those used to prepare **2a**,**b**, and regardless of the ruthenium:diphosphine stoichiometry, dppb reacts with [(*p*-cymene)$RuCl_2$]$_2$ to afford the diphosphine-bridged dimer [{(*p*-cymene)-$RuCl_2$}$_2$(μ-dppb)] (**6**) (eq 2), the identity of which was unequivocally established by a single-crystal X-ray study (vide infra).

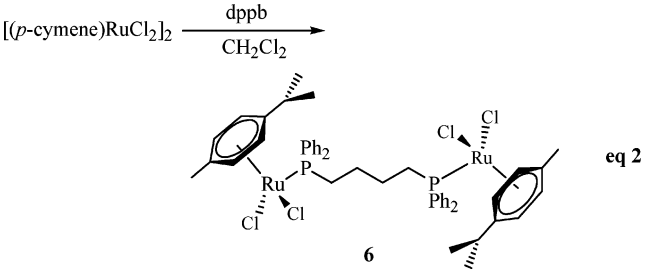

eq 2

The chemical shift of δ 24.8 in the ^{31}P NMR spectrum of **6** is similar to that of 25.0 reported for [{(C_6H_6)-$RuCl_2$}]$_2$(μ-dppb),[26] while the intensities of the resonances associated with methylene protons of dppb relative to the aromatic signals of the *p*-cymene fragment are entirely consistent with this dimeric formulation. Formation of **6** is perhaps not surprising, since there are a number of reports of four-carbon-bridged diphosphines such as dppb and DIOP that bridge two ruthenium atoms. For instance, the reaction of dppb and DIOP with [(C_6H_6)$RuCl_2$]$_2$ to give [{(C_6H_6)$RuCl_2$}$_2$(μ-dppb)] and [{(C_6H_6)$RuCl_2$}$_2$(μ-DIOP)], respectively, reported by James and co-workers,[26] is particularly relevant, as is the reaction between dppb and the bis(allyl) dimer [{Ru(η^3:η^3:$C_{10}H_{16}$)(μ-Cl)Cl}$_2$] to afford [{Ru(η^3:η^3:$C_{10}H_{16}$)Cl_2}$_2$(μ-dppb)].[27]

Although we have previously shown that the ruthenium complex [$RuCl_2$(1,2,3,4-Me_4-NUPHOS)(en)] rapidly dissociates a chloro ligand in chloroform to give [RuCl(*P*,*P*,η^2(*C*)-1,2,3,4-Me_4-NUPHOS)(en)]Cl and that these two complexes cleanly and quantitatively interconvert in a solvent-dependent equilibrium that involves reversible formation of six-electron-donor NUPHOS diphosphines, we found no evidence for such a process occurring with **2a**,**b**, in either dichloromethane, THF, chloroform, or methanol.[20] However, the chloro ligand in **2a,b** can be abstracted by reaction with a slight excess of $AgSbF_6$ to afford [(*p*-cymene)Ru(*P*,*P*,η^2(*C*)-NUPHOS)][SbF_6]$_2$ (**3a**,**b**), in which one of the C=C double bonds of the butadiene tether is coordinated in an η^2-manner to the metal center (Scheme 1). Definitive evidence for the presence of the *P*,*P*,η^2(*C*)-coordinated

(25) den Reijer, C. J.; Drago, D.; Pregosin, P. S. *Organometallics* **2001**, *20*, 2982.

(26) Fogg, D. E.; James, B. R. *J. Organomet. Chem.* **1993**, *462*, C21.

(27) Cadierno, V.; Garcia-Garrido, S. E.; Gimeno, J. *Inorg. Chim. Acta*. **2003**, *347*, 41.

diphosphine was provided by the distinctive ^{31}P NMR spectrum, which contained two well-separated pairs of doublets, one at δ 78.9 (**3a**), 82.1 (**3b**) and the other at much higher field, δ 6.5 (**3a**), 9.0 (**3b**), the latter in the region expected for a $P,P,\eta^2(C)$-coordinated diphosphine and associated with the diphenylphosphino group adjacent to the coordinated double bond. Since Pregosin has warned against relying on ^{31}P NMR spectroscopy as the sole technique for identifying this type of interaction,[22,23a] C−H long-range correlation was also used to unequivocally assign the resonances associated with the carbon atoms of the η^2-coordinated double bond. In the case of **3a**, long-range correlation identified a doublet at δ 62 and a doublet of doublets at δ 102, which we confidently assign to the two carbon atoms of the η^2-coordinated double bond. These resonances show two and three cross-peaks, respectively, which arise from two- and three-bond J(C−H) coupling to the protons of neighboring methyl groups. The doublet at δ 62 clearly correlates with only two sets of methyl protons, a singlet and a doublet, and must therefore belong to the carbon bonded to phosphorus, while the doublet of doublets at δ 102 shows cross-peaks to three sets of methyl protons, two singlets and a doublet. This long-range correlation study can also be used to assign the two carbon atoms associated with the uncoordinated double bond. In a similar manner the pattern of cross-peaks in the C−H long-range correlation of **3b** has been used to identify each of the carbon atoms of the monocyclic NUPHOS tether.

While the chloro ligand in **2a** was readily abstracted under mild reaction conditions, that in **4a**,**b** proved much more difficult to remove, so much so that it was impossible to isolate pure samples of the corresponding 6e-donor BIPHEP and MeO-BIPHEP complexes [(*p*-cymene)Ru(BIPHEP)][SbF_6]$_2$ (**5a**) and [(*p*-cymene)Ru(MeO-BIPHEP)][SbF_6]$_2$ (**5b**), respectively. Typically, treatment of a dichloromethane solution of [(*p*-cymene)Ru(BIPHEP)Cl][SbF_6] (**4a**) or [(*p*-cymene)Ru(MeO-BIPHEP)Cl][SbF_6] (**4b**) with an excess of $AgSbF_6$ gave a 30:70 mixture of **5a**,**b** and **4a**,**b** even after heating at reflux for 12 h. In each case a ^{31}P NMR spectrum of the crude reaction mixture clearly showed two sets of signals, a major pair of doublets corresponding to unreacted **4a/b** together with two minor exchange-broadened signals at ca. δ 65 and 3 associated with **5a/b**. In stark contrast, the formation of **3a**,**b** occurs rapidly and quantitatively under mild conditions, i.e., in dichloromethane at room temperature. Such facile conversion of a four-electron NUPHOS diphosphine into its six-electron $P,P,\eta^2(C)$-coordinated counterpart is consistent with our previous studies in which [$RuCl_2$(1,2,3,4-Me_4-NUPHOS)(en)] (en = ethylenediamine) rapidly dissociates chloride in chloroform to give [RuCl($P,P,\eta^2(C)$-1,2,3,4-Me_4-NUPHOS)(en)][Cl] (eq 1), whereas its BINAP counterpart is indefinitely stable in solution.[20] Thus, NUPHOS-type diphosphines clearly demonstrate a much greater propensity to coordinate in a $P,P,\eta^2(C)$-manner than BINAP, BIPHEP, or MeO-BIPHEP, which we tentatively suggest to be associated with an inherently greater conformational flexibility of the 1,3-butadiene tether as well as an intrinsically more favorable η^2-coordination of the butadiene fragment compared with the aromatic system of a biaryl fragment.

The reaction of **3a** with pyridine was examined in an attempt to demonstrate that the C=C double bond of the $P,P,\eta^2(C)$-coordinated NUPHOS was of sufficient substitutional lability to form the dication [(*p*-cymene)-Ru(1,2,3,4-Me_4-NUPHOS)(py)][SbF_6]$_2$. However, rather than forming the desired adduct, addition of pyridine to a dichloromethane solution of **3a**, generated in situ by abstraction of chloride from **2a** with $AgSbF_6$, resulted in rapid and quantitative hydrolysis to afford [(*p*-cymene)Ru{Ph_2(O)PC(H)MeCMeCMeCMePPh_2}]-[SbF_6] (**7**), which was initially identified by a combination of ^1H NMR spectroscopy and FAB mass spectrometry and subsequently by a single-crystal X-ray study (eq 3). Two low-field singlets at δ 73.4 and 68.5 in the ^{31}P NMR spectrum of **7** are consistent with a small or zero $^3J_{PP}$ for a *P*,*O*-coordinated bis(phosphine)monoxide, as observed for Pd, Pt, Rh, and most recently ruthenium complexes of BINAP monoxide. Several unusual features in the ^1H NMR spectrum of **7** provided the first indication that an unexpected transformation had occurred. In particular, a low-field doublet of quartets of intensity 1H at δ 5.02 corresponds to the methine proton of the newly formed CHMe adjacent to the phosphine oxide, while its methyl substituent appears as a doublet of doublets at δ 1.53. As expected, the methyl groups at the 2- and 3-positions of the butadiene tether appear as singlets at δ 1.15 and 0.73, and the remaining methyl group adjacent to the diphenylphosphino fragment appears as a doublet at δ 1.45. The most likely origin of the adventitious water involved in this transformation is the pyridine, which was not dried prior to use, the pyridine acting to remove the $HSbF_6$ generated during the hydrolysis. In a comparative series of experiments compound **3a** did not react with dry pyridine to form the desired adduct [(*p*-cymene)Ru(1,2,3,4-Me_4-NUPHOS)(py)][SbF_6]$_2$, nor did it undergo hydrolysis in the absence of pyridine. Overall, formation of **7** involves oxidation of one of the diphenylphosphino groups and a highly selective syn addition of Ru and H across the double bond of the butadiene tether adjacent to the phosphine oxide, presumably via a hydride intermediate.

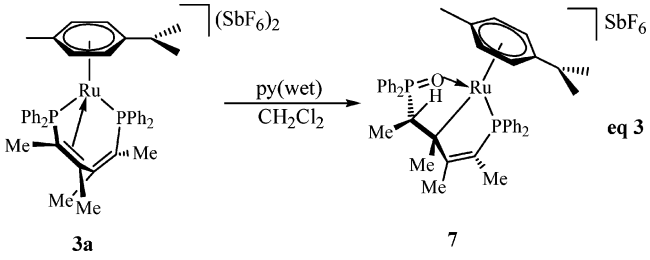

Crystal Structures of [(*p*-cymene)Ru(1,2,3,4-Me_4-NUPHOS)Cl][ClO_4] (2a), [(*p*-cymene)Ru(1,4-Et_2-2,3-*cyclo*-C_6H_8-NUPHOS)Cl][SbF_6] (2b), [(*p*-cymene)-Ru($P,P,\eta^2(C)$-1,2,3,4-Me_4-NUPHOS)][SbF_6]$_2$ (3a), [(*p*-cymene)Ru(BIPHEP)Cl][SbF_6] (4a), [{(*p*-cymene)-$RuCl_2$}$_2$(μ-dppb)] (6), and [(*p*-cymene)Ru{Ph_2(O)-PC(H)MeCMeCMeCMePPh_2}][SbF_6] (7). The marked difference in reactivity between **2a**,**b** and **4a**, particularly with respect to halide abstraction, prompted us to undertake single-crystal X-ray analyses of each of these compounds, the molecular structures of which are shown in Figures 1−3, with selected bond lengths and

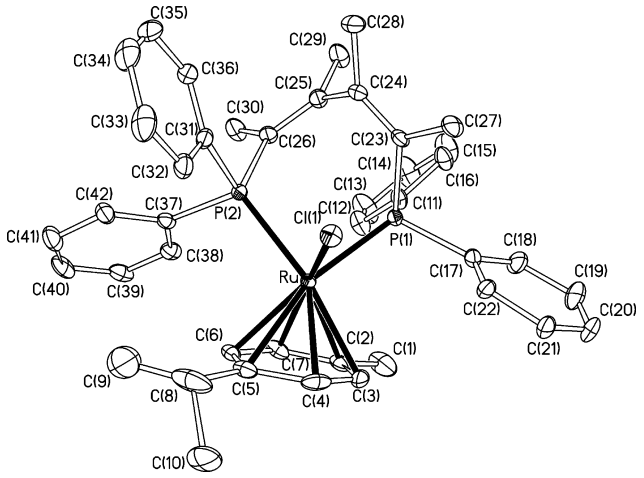

Figure 1. Molecular structure of [(*p*-cymene)Ru(1,2,3,4-Me_4-NUPHOS)Cl][ClO_4] (**2a**). Hydrogen atoms, dichloromethane molecules of crystallization, minor disorder components, and the perchlorate anion have been omitted for clarity. Ellipsoids are at the 30% probability level.

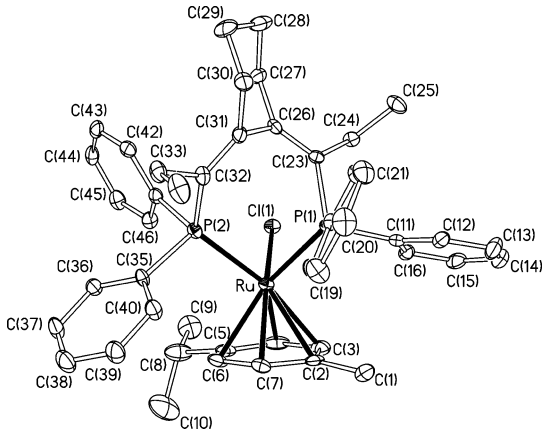

Figure 2. Molecular structure of [(*p*-cymene)Ru(1,4-Et_2-2,3-*cyclo*-C_6H_8-NUPHOS)Cl][SbF_6] (**2b**). Hydrogen atoms, chloroform molecules of crystallization, and the hexafluoroantimonate anion have been omitted for clarity. Ellipsoids are at the 30% probability level.

angles listed in Table 1 and crystal data presented in Table 4. Since the structures of each of these compounds are based on *p*-cymene ruthenium complexes of C_4-bridged *tropos* diphosphines and are clearly related, they will be described together. The coordination of the metal is similar in all complexes and is best described as octahedral, with three sites occupied by the η^6-*p*-cymene fragment and the remaining three by two diphenylphosphino groups and a chloro ligand. The six Ru−C(arene) distances in all three complexes fall between 2.247(7) and 2.345(6) Å and are within the range expected on the basis of related complexes such as [(arene))Ru(BINAP)Cl]$^+$,[27,28] [(*p*-cymene)Ru(BDPBzP)I]I,[29] and [(*p*-cymene)Ru(dppf)Cl][PF_6].[30] The natural bite angles of 88.50(3)° (**2a**), 87.05(6)° (**2b**), and 89.68(7)° (**4a**) are comparable to those reported for

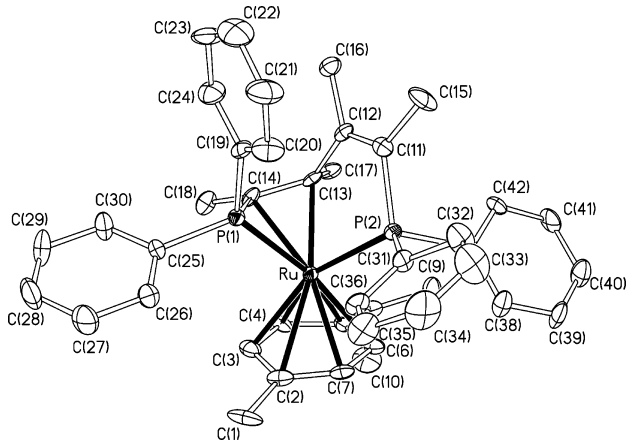

Figure 3. Molecular structure of [(*p*-cymene)Ru(1,2,3,4-Me_4-NUPHOS)][SbF_6]$_2$ (**3a**), illustrating the *P,P*,η^2(*C*)-coordination of Me_4-NUPHOS. Hydrogen atoms and hexafluoroantimonate anions have been omitted for clarity. Ellipsoids are at the 30% probability level.

related complexes of C_4-bridged biaryl diphosphines,[31] as are the corresponding Ru−P distances, which lie between 2.335(2) and 2.4082(17) Å. The Ru−Cl bond lengths are also unexceptional, with that of 2.3976(18) Å in **4a** slightly shorter than those of 2.4114(13) and 2.4056(10) Å in **2b** and **2a**, respectively. The dihedral angle of 66.7° between the least-squares plane containing the two sp^2-carbon atoms and their substituents in **2a** is slightly larger than the corresponding angles of 60.1° and 60.7° in **2b** and **4a**, respectively.

A single-crystal X-ray structure determination of **3a** has also been undertaken in order to determine the influence of *P,P*,η^2(*C*)-coordination on the metal−diphosphine bonding and coordination geometry at the metal center. A perspective view of the molecular structure of **3a** is shown in Figure 3, and a selection of bond lengths and angles is listed in Table 3. The structure reveals that the NUPHOS diphosphine coordinates in a *P,P*,η^2(*C*)-manner and occupies a facial coordination environment, bonded through both phosphorus atoms and one of the double bonds of the butadiene tether. The remaining facial coordination sites are occupied by the η^6-*p*-cymene fragment, which exhibits a marked deviation from planarity with C(2) and C(5) displaced by 0.0574 and 0.0456 Å, respectively, out of the mean plane of the six carbon atoms. The C(13)−C(14) bond length of 1.441(11) Å shows the elongation expected upon η^2-coordination[32] compared with that of 1.311(11) Å for the uncoordinated double bond C(11)−C(12). The Ru−C(13) and Ru−C(14) bond lengths of 2.237(7) and 2.211(7) Å are very similar, as has previously been noted for the related complex [(η^6-

(28) Mashima, K.; Kusano, K.; Sato, N.; Matsumara, Y.; Nozaki, K.; Kumobayashi, H.; Hori, Y.; Ishizaki, T.; Akutagawa, S.; Takaya, H. *J. Org. Chem*. **1994**, *59*, 3064.

(29) Bianchini, C.; Barbaro, P.; Scapacci, G.; Zanobini, F. *Organometallics* **2000**, *19*, 2450.

(30) Jensen, S. B.; Rodger, S. J.; Spicer, M. D. *J. Organomet. Chem*. **1998**, *556*, 151.

(31) (a) Tudor, M. D.; Becker, J. J.; White, P. S. Gagné, M. R. *Organometallics* **2000**, *19*, 4376. (b) Tominaga, H.; Sakai, K.; Tsubomura, T. *J. Chem. Soc., Chem. Commun*. **1995**, 2273. (c) Wicht, D. K.; Zhuravel, M. A.; Gregush, R. V.; Glueck, D. S.; Guzei, I. A.; Liable-Sands, L. M.; Rheingold, A. L. *Organometallics* **1998**, *17*, 1412. (d) Alcock, N. W.; Brown, J. M.; Perez-Torrente, J. *Tetrahedron Lett*. **1992**, *33*, 389. (e) Brown, J. M.; Perez-Torrente, J. J.; Alcock, N. W. *Organometallics* **1995**, *14*, 1195. (f) Motoyama, Y.; Murata, K.; Kurihara, O.; Naitoh, T.; Aoki, K.; Nishiyama, H. *Organometallics* **1998**, *17*, 1251. (g) Motoyama, Y.; Kurihara, O.; Murata, K.; Aoki, K.; Nishiyama, H. *Organometallics* **2000**, *19*, 1025.

(32) (a) Motoyama, Y.; Murata, K.; Kurihara, O.; Naitoh, T.; Aoki, K.; Nishiyama, H. *Organometallics* **1998**, *17*, 1251. (b) Motoyama, Y.; Kurihara, O.; Murata, K.; Aoki, K.; Nishiyama, H. *Organometallics* **2000**, *19*, 1025.

Table 1. Selected Bond Distances (Å) and Angles (deg) for 2a, 2b, and 4a

compound **2a**		compound **2b**		compound **4a** (molecule a)	
Ru−P(1)	2.3526(12)	Ru−P(1)	2.3450(15)	Ru(1)−P(1)	2.340(2)
Ru−P(2)	2.3944(9)	Ru−P(2)	2.4081(16)	Ru(1)−P(2)	2.3732(19)
Ru−Cl(1)	2.4056(10)	Ru−Cl(1)	2.4114(13)	Ru(1)−Cl(11)	2.3976(18)
Ru−C(2)	2.299(4)	Ru−C(2)	2.331(6)	Ru(1)−C(2)	2.303(8)
Ru−C(3)	2.267(4)	Ru−C(3)	2.300(6)	Ru(1)−C(3)	2.284(8)
Ru−C(4)	2.265(4)	Ru−C(4)	2.268(6)	Ru(1)−C(4)	2.265(7)
Ru−C(5)	2.311(4)	Ru−C(5)	2.343(6)	Ru(1)−C(5)	2.344(7)
Ru−C(6)	2.266(4)	Ru−C(6)	2.284(6)	Ru(1)−C(6)	2.265(7)
Ru−C(7)	2.270(4)	Ru−C(7)	2.288(6)	Ru(1)−C(7)	2.247(7)
C(23)−C(24)	1.352(5)	C(23)−C(26)	1.342(8)	C(23)−C(28)	1.391(10)
C(24)−C(25)	1.489(6)	C(26)−C(31)	1.509(8)	C(28)−C(29)	1.512(10)
C(25)−C(26)	1.350(5)	C(31)−C(32)	1.337(8)	C(29)−C(30)	1.402(10)
C(2)−C(3)	1.422(7)	C(2)−C(3)	1.434(9)	C(2)−C(3)	1.403(11)
C(3)−C(4)	1.359(7)	C(3)−C(4)	1.427(10)	C(3)−C(4)	1.376(10)
C(4)−C(5)	1.456(6)	C(4)−C(5)	1.425(10)	C(4)−C(5)	1.436(10)
C(5)−C(6)	1.402(6)	C(5)−C(6)	1.407(9)	C(5)−C(6)	1.395(10)
C(6)−C(7)	1.428(6)	C(6)−C(7)	1.412(9)	C(6)−C(7)	1.403(10)
C(7)−C(2)	1.398(6)	C(7)−C(2)	1.411(9)	C(7)−C(2)	1.422(10)
P(1)−Ru−P(2)	88.50(3)	P(1)−Ru−P(2)	87.01(5)	P(1)−Ru(1)−P(2)	89.68(7)
P(1)−Ru−Cl(1)	84.32(4)	P(1)−Ru−Cl(1)	85.11(5)	P(1)−Ru(1)−Cl(11)	84.61(7)
P(2)−Ru−Cl(1)	89.75(3)	P(2)−Ru−Cl(1)	90.29(5)	P(2)−Ru(1)−Cl(11)	90.14(7)
P(1)−C(23)−C(24)	118.4(3)	P(1)−C(23)−C(26)	120.3(4)	P(1)−C(23)−C(28)	121.9(5)
C(23)−C(24)−C(25)	125.1(4)	C(23)−C(26)−C(31)	126.5(5)	C(23)−C(28)−C(29)	124.2(6)
C(24)−C(25)−C(26)	127.2(3)	C(26)−C(31)−C(32)	128.0(5)	C(28)−C(29)−C(30)	127.9(6)
C(25)−C(26)−P(2)	120.9(3)	C(31)−C(32)−P(2)	121.1(4)	C(29)−C(30)−P(2)	123.8(5)

Table 2. Selected Bond Distances (Å) and Angles (deg) for 3a

Ru−P(1)	2.315(2)	C(11)−C(12)	1.311(11)
Ru−P(2)	2.315(2)	C(12)−C(13)	1.499(11)
Ru−C(2)	2.355(9)	C(13-C(14)	1.441(11)
Ru−C(3)	2.260(8)	C(2)−C(3)	1.402(12)
Ru−C(4)	2.292(7)	C(3)−C(4)	1.410(11)
Ru−C(5)	2.379(8)	C(4)−C(5)	1.400(11)
Ru−C(6)	2.282(8)	C(5)−C(6)	1.435(11)
Ru−C(7)	2.246(8)	C(6)−C(7)	1.420(11)
Ru−C(13)	2.237(7)	C(7)−C(2)	1.337(12)
Ru−C(14)	2.211(7)		
P(1)−Ru−P(2)	91.16(8)	Ru−C(14)−P(1)	69.8(3)
Ru−C(13)−C(17)	117.7(5)	Ru−C(14)−C(18)	122.2(6)
Ru−C(13)−C(12)	114.7(5)	Ru−C(14)−C(13)	72.1(4)
Ru−C(13)−C(14)	70.1(4)	C(14)−Ru−C(13)	37.8(3)

Table 3. Selected Bond Distances (Å) and Angles (deg) for 6

Ru−P	2.3487(9)	C(11)−C(12)	1.374(5)
Ru−Cl(1)	2.4195(8)	C(12)−C(13)	1.391(5)
Ru−Cl(2)	2.4140(8)	C(13)−C(14)	1.376(7)
Ru−C(2)	2.217(3)	C(2)−C(3)	1.413(5)
Ru−C(3)	2.159(3)	C(3)−C(4)	1.403(5)
Ru−C(4)	2.182(3)	C(4)−C(5)	1.421(5)
Ru−C(5)	2.213(3)	C(5)−C(6)	1.424(5)
Ru−C(6)	2.245(3)	C(6)−C(7)	1.395(5)
Ru−C(7)	2.234(3)	C(7)−C(2)	1.426(5)
P−Ru−Cl(1)	83.04(3)	Cl(1)−Ru−Cl(2)	88.30(3)
P−Ru−Cl(2)	88.44(3)		

indole)Ru(MeO-BIPHEP-Bu)][BF_4]$_2$ [2.34(3) and 2.31(3) Å]. The dihedral angle of 75.7° between the least-squares planes defined by C(13)C(14)C(17)C(18) and C(11)C(12)C(15)C(16) is significantly larger than that of 66.1° in **2a**, reflecting the dramatic conformational changes experienced upon η^2-coordination of C(13)−C(14). A similar increase in dihedral angle occurs upon changing from *P,P* coordination in [CpRuI(BINAP)] (66°) to *P,P*,η^2-naphthyl coordination in [CpRu(BINAP)] (80°).[21] James has also noted that the dihedral angle of

Table 4. Selected Bond Distances (Å) and Angles (deg) for 7

Ru−P(1)	2.2814(10)	C(2)−C(3)	1.439(6)
Ru−O	2.163(2)	C(3)−C(4)	1.381(6)
Ru−C(25)	2.223(3)	C(4)−C(5)	1.447(6)
Ru−C(2)	2.228(4)	C(5)−C(6)	1.396(6)
Ru−C(3)	2.243(4)	C(6)−C(7)	1.418(6)
Ru−C(4)	2.252(4)	C(7)−C(2)	1.415(6)
Ru−C(5)	2.289(4)	C(23)−C(24)	1.333(5)
Ru−C(6)	2.286(4)	C(24)−C(25)	1.528(5)
Ru−C(7)	2.180(4)	C(25)−C(26)	1.560(5)
P(2)−O	1.514(2)		
P(1)−Ru−O	88.74(7)	O−Ru−C(25)	79.29(11)
P(1)−Ru−C(25)	79.87(9)	P(2)−O−Ru	112.72(13)

81.6° in [RuCl(*P,P*,η^2-naphthyl-BINAPO)(phen)][PF_6] is greater than that of 77.37° in [$RuCl_2$(BINAP)(phen)].[24] The two Ru−P bond lengths are identical [2.315(2) Å] and slightly shorter than those of 2.3944(9) and 2.3526(12) Å in **2a**, which is presumably associated with the additional positive charge on **3a**. Although the natural bite angle of 91.16(8)° is slightly larger than that in **2a**, it falls within the range expected for ruthenium complexes of six-electron-donor diphosphines such as MeO-BIPHEP.[22]

Although the spectroscopic data for **6**, in particular the relative intensities of the resonances in the ^{1}H NMR spectrum, were consistent with its formulation as a dppb-bridged dimer, a single-crystal X-ray study was undertaken to unequivocally confirm its identify, the result of which is shown in Figure 5. A selection of bond lengths and angles is listed in Table 3. The molecular structure clearly shows two (*p*-cymene)$RuCl_2$ fragments connected through a dppb bridge in a piano stool configuration. The two Ru−C bonds that lie trans to the phosphorus atoms, namely, Ru−C(6) (2.245(3) Å) and Ru−C(7) (2.234(3) Å) are slightly longer than the remaining four Ru−C bonds [d(Ru−C)$_{av}$ = 2.193 Å]. Similar bond length patterns have previously been noted for [(C_6H_6)$RuCl_2$($PMePh_2$)] and [(*p*-cymene)$RuCl_2$-

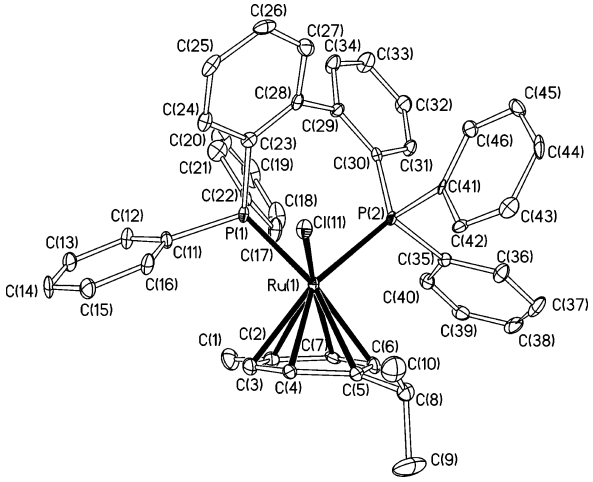

Figure 4. Molecular structure of [(*p*-cymene)Ru(BIPHEP)-Cl][SbF_6] (**4a**). Hydrogen atoms, dichloromethane molecules of crystallization, and the hexafluoroantimonate anion have been omitted for clarity. Ellipsoids are at the 30% probability level.

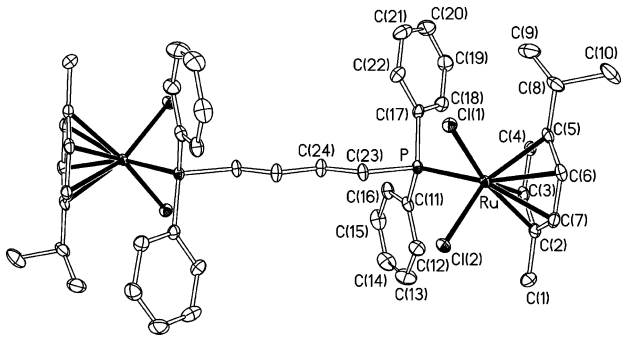

Figure 5. Molecular structure of [{(*p*-cymene)$RuCl_2$}$_2$(μ-dppb)] (**6**). Hydrogen atoms and dichloromethane and hexane molecules of crystallization have been omitted for clarity. Ellipsoids are at the 30% probability level.

($PMePh_2$)][33] and attributed to the bond-lengthening trans effect of the tertiary phosphine ligand. The *p*-cymene ring is essentially planar, with maximum and mean deviations from the least-squares mean plane of the six carbon atoms of −0.0218 and 0.0012 Å, respectively.

Finally, a single-crystal X-ray study of **7** was undertaken to confirm its formulation and to establish the relative stereochemistry of the two new stereocenters. A perspective view of the molecular structure is shown in Figure 6, and selected bond lengths and angles are listed in Table 4. The X-ray study reveals that **7** results from oxidation of one end of 1,2,3,4,Me_4-NUPHOS and regioselective syn addition of Ru and H to the double bond proximate to the newly formed phosphine oxide, to afford a ligand that can most aptly be described as an unsymmetrical bis(phosphine) monoxide pincer, which coordinates in a *P*,*O*,η^1(*C*)-terdentate manner to form two five-membered rings. The Ru−P(1) and Ru−O(1) bond lengths of 2.2814(10) and 2.163(2) Å, respectively, are typical for a bisphosphine monoxide (BPMO) *P*,*O*-coordinated to ruthenium(II),[34] and Ru−C(25) [2.223(3) Å] is within the range expected for a Ru−

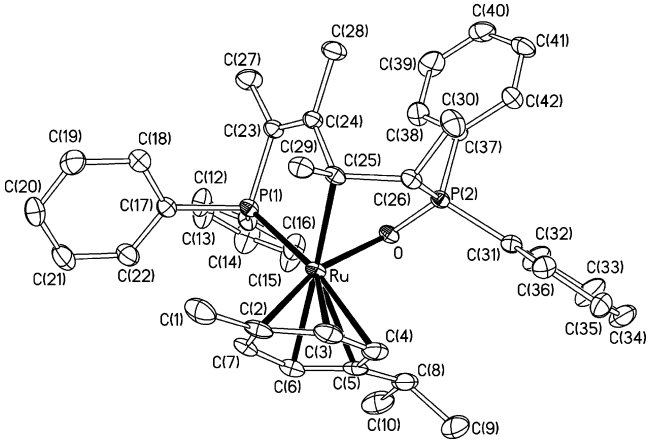

Figure 6. Molecular structure of [(*p*-cymene)Ru{Ph_2(O)-PC(H)MeCMeCMeCM$ePPh_2$}][SbF_6] (**7**). Hydrogen atoms and dichloromethane molecule of crystallization have been omitted for clarity. Ellipsoids are at the 30% probability level.

C(sp^3) σ-bond.[35] The P═O bond length of 1.514(2) Å falls within the range expected for a coordinated phosphine oxide and is very similar to that of 1.493(4) Å in [(*p*-cymene)Ru{*P*,*O*-(*S*)-BINAPO}][SbF_6][34] and 1.518(3) Å in [RuCl(BINAPO)(bipy)][PF_6],[24] and the P(1)−Ru−O(1) bite angle of 88.74(7)° is similar to that of 87.71(12)° in [RuCl(BINAPO)(phen)][PF_6].[24] The Ru−O(1)−P(1) bond angle of 112.72(13)° presumably reflects the size of the chelate ring, since the corresponding angles of 98.6(2)° and 97.2(1)° in [RuCl(BINAPO)(phen)][PF_6] and [RuCl-(BINAPO)(bipy)][PF_6], respectively, are much smaller, which was suggested to be due to η^2-coordination of the two carbon atoms of the naphthyl ring proximate to the P═O group.[24] In contrast, the P═O−M angle in complexes in which BINAPO acts solely as a heterobidentate *P*,*O*-chelate is much larger: 165.9(3)° in [(*p*-cymene)RuCl(*P*,*O*-BINAPO][SbF_6][34] and 161.5(5)° in [(*p*-cymene)OsCl(*P*,*O*-BINAPO][SbF_6].[36]

Catalysis: Ruthenium-Catalyzed Addition of Benzoic Acid to 1-Alkynes. The clear structural similarity between biaryl-based diphosphines such as BIPHEP and NUPHOS-type diphosphines and the ability of both to coordinate to ruthenium in a *P*,*P*,η^2(*C*)-manner prompted us to undertake a comparison of their performance in the ruthenium-catalyzed addition of benzoic acid to terminal alkynes. The regio- and stereoselective addition of carboxylic acids to terminal alkynes has evolved as a highly versatile reaction since the resulting enol esters are important reagents and intermediates in organic synthesis;[37] for example, enol esters resulting from Markovnikov addition are widely used for the acylation of alcohols and amines.[38] More recently the catalytic intramolecular Markovnikov addition of a hydroxy group to an unactivated terminal triple bond has been applied to the synthesis of functional furans[39]

(33) Bennett, M. A.; Robertson, G. B.; Smith, A. K. *J. Organomet. Chem*. **1972**, *43*, C41.
(34) Faller, J. W.; Parr, J. *Organometallics* **2000**, *19*, 1829.
(35) Fang, X.; Watkin, J. G.; Scott, B. L.; John, K. D.; Kubas, G. J. *Organometallics* **2002**, *21*, 2336.
(36) Faller, J. W.; Parr, J. *Organometallics* **2001**, *20*, 697.
(37) (a) Fischmeister, C.; Bruneau, C. Dixneuf, P. H. In *Ruthenium in Organic Synthesis*; Murahashi, S.-I., Ed.; Wiley-VCH: New York, 2004; Chapter 8, p 189. (b) Bruneau, C.; Dixneuf, P. H. *Chem. Commun*. **1997**, 507.
(38) Kita, Y.; Akai, S.; Yoshigi, M.; Nakajima, Y.; Yasuda, H.; Tamura, Y. *Tetrahedron Lett*. **1984**, *25*, 6067.

Table 5. Summary of Crystal Data and Structure Determination for 2a, 2b, 3a, 4a, 6, and 7

	2a	2b	3a	4a	6	7
formula	$C_{42}H_{46}ClP_2Ru^+ \cdot ClO_4^- \cdot 2CH_2Cl_2$	$C_{46}H_{52}ClP_2Ru^+ \cdot SbF_6^- \cdot 2CHCl_3$	$C_{42}H_{46}P_2Ru^{2+} \cdot 2SbF_6^- \cdot CH_2Cl_2$	$C_{46}H_{42}P_2ClRu^+ \cdot SbF_6^- \cdot 2CH_2Cl_2$	$C_{48}H_{56}P_2Ru_2 \cdot 2CH_2Cl_2 \cdot C_6H_{14}$	$C_{42}H_{47}OP_2Ru^+ \cdot SbF_6^- \cdot CH_2Cl_2$
fw	1018.6	1277.8	1270.2	1198.9	1294.8	1051.5
cryst syst	monoclinic	monoclinic	monoclinic	triclinic	triclinic	monoclinic
space group	$P2_1$	$P2_1/c$	$C2/c$	$P\bar{1}$	$P\bar{1}$	$P2_1/c$
T (K)	150	150	150	150	150	150
a (Å)	13.564(3)	10.1035(5)	24.3186(11)	14.7948(13)	10.4797(5)	11.2957(15)
b (Å)	14.897(3)	28.610(5)	29.7261(13)	17.8716(15)	11.8099(14)	13.4324(11)
c (Å)	13.853(3)	18.303(5)	16.5645(7)	19.9255(17)	13.5696(12)	31.891(3)
α (deg)				97.429(1)	92.326(9)	
β (deg)	117.49(3)	97.250(6)	123.608(1)	94.401(2)	108.030(5)	96.170(13)
γ (deg)				111.458(1)	112.768(8)	
V (Å^3)	2483.1(9)	5248.4(16)	9972.8(8)	4818.0(7)	1447.7(2)	4810.8(9)
Z	2	4	8	4	1	4
reflns measd	99 089	94 570	34 471	34 205	20 141	57 077
unique data, R_{int}	11 363, 0.0501	9109, 0.0637	8765, 0.0708	34 205	6574, 0.0396	10 946, 0.0630
params	519	556	555	1167	283	486
R (F, $F^2 > 2\sigma$)	0.0403	0.0569	0.0627	0.0714	0.0413	0.0474
R_w (F^2, all data)	0.1153	0.1599	0.1509	0.2019	0.1035	0.1390
GOF on F^2	1.114	1.108	1.038	1.022	1.039	1.074
max., min. electron density (e/Å^3)	0.67, −0.45	0.99, −0.72	1.28, −1.36	2.29, −1.68	0.78, −1.00	0.93, −1.02

and enol lactones[40] while anti-Markovnikov addition has been used for the synthesis of functional dienes and aldehydes.[37]

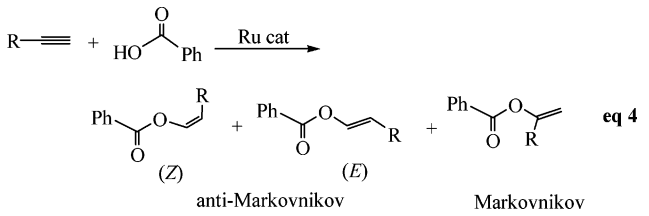

eq 4

Preliminary results for addition of benzoic acid to 1-pentyne, 1-octyne, and phenylacetylene (eq 4) using catalysts based on Me_4-NUPHOS, 1,4-Et_2-2,3-*cyclo*-C_6H_8-NUPHOS, and dppb, as well as BIPHEP and MeO-BIPHEP for comparison, are summarized in Table 6. Catalysts were typically generated in situ by abstraction of chloride from the corresponding precursor with $AgSbF_6$ prior to addition of substrate, since crystalline samples of the six-electron-donor dications are generally very insoluble in the small volume of solvent used to perform the catalysis. In the case of 1-octyne, comparative testing was also conducted with catalyst generated by activation of $[(p\text{-cymene})RuCl_2]_2$ with $AgSbF_6$ in order to evaluate the influence of the diphosphine. Prior to this study, Pregosin has previously reported that the dication $[(p\text{-cymene})Ru(\text{MeO-BIPHEP})][SbF_6]_2$ catalyzes the highly regioselective addition of benzoic acid to 1-pentyne and 1-octyne under mild conditions to give the anti-Markovnikov addition product with a cis-to-trans ratio of 70:30 and that the same catalyst was completely inactive for addition to phenylacetylene (vide infra). All three alkynes were reported to react with $[(p\text{-cymene})Ru(\text{MeO-BIPHEP})][SbF_6]_2$ via cyclometalation-alkyne insertion to afford **8** as the thermodynamic product (eq 5). However, while the 1-pentyne and 1-octyne insertion products both catalyzed hydrocarboxylation, the product of phenylacetylene insertion was reported to be stable with respect to further reaction.[25]

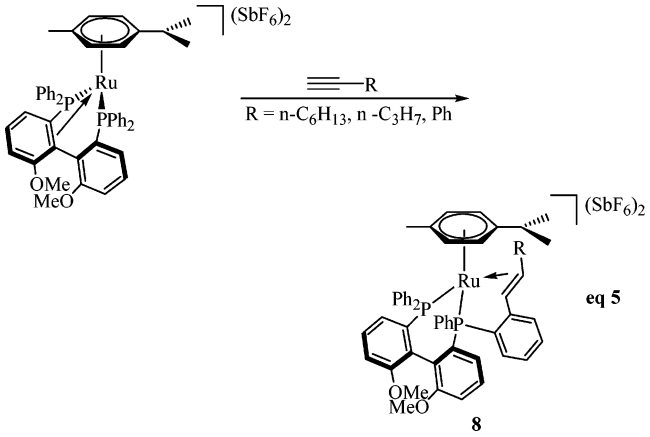

eq 5

The dication generated by activation of **2a** with $AgSbF_6$ catalyzes the highly regioselective anti-Markovnikov addition of benzoic acid to both 1-pentyne and 1-octyne to give the corresponding alk-1-en-1-yl ester with a cis-to-trans ratio of 92:8 and no evidence for the Markovnikov addition product (entries 2 and 6). For comparison, under the same conditions the MeO-BIPHEP-based catalyst also gave the anti-Markovnikov addition product exclusively, but with a significantly lower stereoselectivity of 70:30 (entry 12), consistent with the performance first reported by Pregosin.[25] Surprisingly, catalyst performance was found to be highly sensitive to 6,6′-substitution of the biaryl tether, since replacement of MeO-BIPHEP with its tropos counterpart BIPHEP resulted in a marked improvement in the cis-to-trans ratio from 70:30 to 85:15 (entry 10). Such a dramatic dependence of selectivity on the biaryl substitution prompted us to investigate the influence of the NUPHOS tether by comparing the performance of catalysts generated from acyclic and monocyclic NUPHOS diphosphines, **2a** and **2b**, respectively. The cis-to-trans ratio of 66:8 for addition to 1-pentyne catalyzed by **2b**/$AgSbF_6$ (entry 4) was markedly lower than that of 92:8 obtained with its Me_4-NUPHOS counterpart, as was that of 66:11 for addition to 1-octyne

(39) (a) Seiller, B.; Bruneau, C.; Dixneuf, P. H. *Tetrahedron* **1995**, *51*, 13089. (b) Seiller, B.; Bruneau, C.; Dixneuf, P. H. *Chem. Commun*. **1994**, 493.

(40) Jimenez Tenorio, M.; Puerta, M. C.; Valerga, P.; Moreno-Dorado, F. J.; Guerra, F. M.; Massanet, G. M. *Chem. Commun*. **2001**, 2324.

Table 6. Ruthenium-Catalyzed Addition of Benzoic Acid to Terminal Alkynes

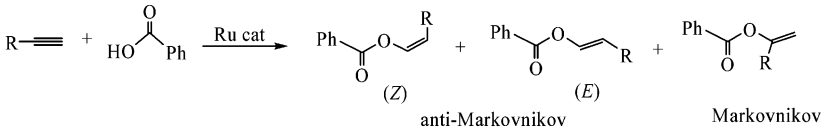

entry[a]	catalyst/ precursor	R	enol ester distribution (%)			Yield (%)[b]
			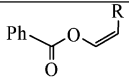	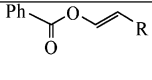	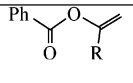	
1	**2a**	C_3H_7	95	5	-	39
2	**2a**/$AgSbF_6$	C_3H_7	92	8	-	38
3	**2b**	C_3H_7	86	7	7	9
4	**2b**/$AgSbF_6$	C_3H_7	66	8	26	18
5	**2a**	C_6H_{13}	94	6	-	78
6	**2a**/$AgSbF_6$	C_6H_{13}	92	8	-	64
7	**2b**	C_6H_{13}	90	10	-	49
8	**2b**/$AgSbF_6$	C_6H_{13}	66	11	23	65
9	**4a**	C_6H_{13}	74	4	22	4
10	**4a**/$AgSbF_6$	C_6H_{13}	85	15	-	69
11	**4b**	C_6H_{13}	86	14	-	69
12	**4b**/$AgSbF_6$	C_6H_{13}	70	30	-	58
13	**6**	C_6H_{13}	19	14	67	12
14	**6**/$AgSbF_6$	C_6H_{13}	5	4	91	78
15	[(*p*-cymene)$RuCl_2$]$_2$/$AgSbF_6$	C_6H_{13}	44	22	34	12
16	**2a**	C_6H_5	95	5	-	85
17	**2a**/$AgSbF_6$	C_6H_5	99	1	-	85
18	**2b**	C_6H_5	77	23	-	66
19	**2b**/$AgSbF_6$	C_6H_5	86	14	-	46
20	**4a**/$AgSbF_6$	C_6H_5	93	5	2	36
21	**4b**/$AgSbF_6$	C_6H_5	89	9	2	42

[a] Reaction conditions: 5 mol % of catalyst, benzoic acid (0.87 mmol), and alkyne (0.99 mmol) in 1.0 mL of $C_2H_4Cl_2$, 25 °C, 96 h (1-pentyne); 60 °C, 24 h (1-ocytne); 60 °C, 20 h (phenylacetylene). [b] Combined isolated yields after purification by column chromatography. Average of three runs.

(entry 8). However, it should be noted that these cis-to-trans ratios are still significantly higher than that of 70:30 obtained with MeO-BIPHEP. More surprising was the marked difference in regioselectivity between catalysts generated from **2a** and **2b**, the former giving anti-Markovnikov addition product exclusively, while the latter gave 23 and 26% of the Markovnikov addition to 1-octyne and 1-pentyne, respectively. Dixneuf has studied the effect of varying the length of the tether in diphosphines of type $Ph_2P(CH_2)_nPPh_2$ ($n = 1-4$) on the addition of carboxylic acids to terminal alkynes and established that catalysts based on 1,4-bis(diphenylphosphino)butane give optimum selectivity for anti-Markovnikov addition (95%), while those based on dppm, dppe, and dppp are less selective, with dppm giving 80% selectivity for Markovnikov addition.[41] Interestingly, both compounds **2a**,**b** are active for the hydrocarboxylation of terminal alkynes in the absence of silver salt, which is somewhat unexpected, since abstraction of halide was considered to be necessary to generate the active 16-electron species **3a**,**b**, albeit stabilized by weak coordination of the butadiene double bond. In fact, the performance of **2a** in the absence of silver salt was comparable to that obtained when activated with $AgSbF_6$ (entries 1 and 5 versus 2 and 6). In contrast, in the absence of silver salt **2b** gave markedly higher regio- and stereoselectivities for addition to both 1-pentyne and 1-octyne than its $AgSbF_6$-activated counterpart. In this regard, Goossen recently reported that addition of silver nitrate to catalyst mixtures generated from [(*p*-cumene)$RuCl_2$]$_2$ and either PPh_3 or P(furyl)$_3$ resulted in a significant enhancement in activity, while maintaining the same selectivity for Markovnikov addition.[42]

Unfortunately, we have been unable to prepare the corresponding dppb-based catalyst precursor [(*p*-cymene)Ru(dppb)Cl][SbF_6] to carry out a direct comparison with **2a**,**b**, since reaction between [(*p*-cymene)-$RuCl_2$]$_2$ and dppb in the presence of $NaSbF_6$ resulted in the rapid formation of a dark brown intractable solid.

(41) Doucet, H.; Martin-Vaca, B.; Bruneau, C.; Dixneuf, P. H. *J. Organomet. Chem*. **1995**, *60*, 7247.

(42) Goossen, L. J.; Paetzold, J.; Koley, D. *Chem. Commun*. **2003**, 706.

However, the dppb-bridged dimer [{(*p*-cymene)$RuCl_2$}$_2$-(μ-dppb)] (**6**) has been isolated as the sole product of reaction in the absence of sodium salt. Catalyst mixtures generated by activation of **6** with $AgSbF_6$ were highly selective for Markovnikov addition to 1-octyne, affording 91% of the oct-1-en-2-yl benzoate together with trace quantities of the anti-Markovnikov addition product (entry 14). Even in the absence of silver salt, **6** catalyzed the Markovnikov hydrocarboxylation of 1-octyne, albeit giving much lower yields of product (entry 13). This reversal of regioselectivity is consistent with **6** acting as 2 equiv of a mono-phosphine-based catalyst, i.e. in much the same manner as [(arene)Ru(PR_3)Cl_2]; such catalysts are highly selective for Markovnikov addition to phenylacetylene and propyne.[43] Goossen et al. have recently demonstrated that catalysts generated in situ from [(*p*-cumene)$RuCl_2$]$_2$ and a monodentate phosphine are highly selective and give up to 97% Markovnikov addition, the best yields being obtained with tri-2-furyl phosphine and an additive such as a silver salt or an inorganic base. The regioselectivity was reversed in the presence of organic bases such as pyridines, which gave 99% selectivity for anti-Markovnikov addition. To demonstrate the influence of the phosphine on catalyst performance, we investigated the hydrocarboxylation of 1-octyne in the presence of catalyst generated by activation of [(*p*-cymene)$RuCl_2$]$_2$ with $AgSbF_6$ and obtained 66% selectivity for anti-Markovnikov addition with a 2:1 ratio of the resulting (*E*)- and (*Z*)-oct-1-en-1-yl benzoate and in low overall yield (entry 15).

To complete a comparative study between the performance of catalysts generated from **2a**,**b** with those based on BIPHEP/MeO-BIPHEP, we have also investigated the hydrocarboxylation of phenylacetylene and found that catalyst mixtures generated by activation of **2a** or **2b** with 1 equiv of $AgSbF_6$ are highly active and regioselective for anti-Markovnikov addition, giving up to 99% selectivity for (*Z*)-styryl benzoate (entries 17 and 19). Interestingly, in an earlier report Pregosin claimed that [(*p*-cymene)Ru(MeO-BIPHEP)][SbF_6]$_2$ was inactive for addition of benzoic acid to phenylacetylene, reasoning that the stability of the cyclometalation-phenylacetylene insertion product **8** was responsible for this inactivity, as it did not react further to afford organic products, while the corresponding 1-octyne insertion product was capable of catalyzing the corresponding addition reaction. Intrigued by such a dramatic difference in catalyst performance for a seemingly minor change in catalyst architecture, we performed the hydrocarboxylation of phenylacetylene and found that, in our laboratory, catalyst mixtures generated by activation of **4a**,**b** with $AgSbF_6$ were highly selective for anti-Markovnikov addition, giving (*Z*)-styryl benzoate as the major enol ester (entries 20 and 21) and only trace amounts (ca. 2%) of the Markovnikov addition product. Although the highly regio- and stereoselective anti-Markovnikov hydrocarboxylation of phenylacetylene using catalysts formed from **4a**,**b** is contrary to an earlier report from the Pregosin group, it should be noted that the catalysts involved in our study were generated in situ and the yields of enol ester are significantly lower than those obtained with catalysts formed from **2a**,**b**.

(43) (a) Ruppin, C.; Dixneuf, P. H.; Lecolier, S. *Tetrahedron Lett*. **1988**, *27*, 5365. (b) Kabouche, Z.; Bruneau, C.; Dixneuf, P. H. *Tetrahedron Lett*. **1991**, *32*, 5359. (c) Philippot, K.; Devanne, D.; Dixneuf, P. H. *Chem. Commun*. **1990**, 1119. (d) Ruppin, C.; Dixneuf, P. H. *Tetrahedron Lett*. **1986**, *27*, 6323. (e) Bruneau, C.; Neveux, M.; Kabouche, Z.; Dixneuf, P. H. *Synlett* **1991**, 755.

Conclusions

Abstraction of a chloro ligand from the ruthenium-*p*-cymene complexes [(*p*-cymene)Ru(1,2,3,4-Me_4-NUPHOS)Cl][SbF_6] (**2a**) and [(*p*-cymene)Ru(1,4-Et_2-2,3-*cyclo*-C_6H_8-NUPHOS)Cl][SbF_6] (**2b**) occurs rapidly and quantitatively at room temperature to afford [(*p*-cymene)Ru(*P*,*P*,η^2(*C*)-1,2,3,4-Me_4-NUPHOS)]-[SbF_6]$_2$ (**3a**) and [(*p*-cymene)Ru(*P*,*P*,η^2(*C*)-1,4-Et_2-2,3-*cyclo*-C_6H_8-NUPHOS)][SbF_6]$_2$ (**3b**), respectively, in which the diphosphine is coordinated as a six-electron donor, bonded through both diphenylphosphino groups and one of the double bonds of the butadiene tether. In contrast, complexes of BIPHEP and MeO-BIPHEP are markedly more reluctant to form the corresponding 6e-donor complexes. Compound **3a** rapidly hydrolyses in the presence of pyridine to give [(*p*-cymene)Ru{Ph_2(O)PC-(H)MeCMeCMeCMePPh_2}][SbF_6] (**7**), which contains a new unsymmetrical bisphosphine monoxide pincer ligand formed by oxidation of one of the diphenylphosphino groups of 1,2,3,4-Me_4-NUPHOS and a highly regioselective syn addition of Ru and H across the butadiene double bond proximate to the phosphine oxide. Dications **3a**,**b** are highly efficient catalysts for the regioselective anti-Markovnikov addition of benzoic acid to 1-pentyne and 1-octyne and give the corresponding alk-1-en-1-yl ester with cis-to-trans ratios up to 95:5, markedly higher than that of 70:30 obtained with MeO-BIPHEP-based catalysts. Catalysts **3a**,**b** are also highly active and selective for anti-Markovnikov addition of benzoic acid to phenylacetylene, giving (*Z*)-styryl benzoate in up to 85% yield and 95:5 selectivity. In our hands, catalyst mixtures formed from **4a** or **4b** and $AgSbF_6$ are active for the hydrocarboxylation of phenylacetylene and give the (*Z*)-styryl benzoate as the major enol ester, which was somewhat of a surprise, considering an earlier report by Pregosin claimed that [(*p*-cymene)Ru(MeO-BIPHEP)][SbF_6]$_2$ (**5b**) reacted with phenylacetylene to afford a thermodynamically stable and catalytically inactive insertion/cyclometalation product. This study has revealed marked differences between the coordination chemistry of NUPHOS-based diphosphines and their biaryl-based counterparts, BIPHEP and MeO-BIPHEP, and highlighted potential advantages of using NUPHOS diphosphines for the ruthenium-catalyzed addition of carboxylic acids to alkynes. As a result of these encouraging studies, we have initiated further studies to explore the scope of NUPHOS diphosphines in ruthenium-catalyzed transformations.

Experimental Section

General Procedures. All manipulations involving air-sensitive materials were carried out in an inert atmosphere glovebox or using standard Schlenk line techniques under an atmosphere of nitrogen or argon in oven-dried glassware. Diethyl ether and hexane were distilled from potassium/sodium alloy and dichloromethane, chloroform, and 1,2-dichloroethane from calcium hydride. BIPHEP and MeO-BIPHEP were purchased from Strem, dppb and benzoic acid from Avocado, and the terminal alkynes phenylacetylene, 1-octyne, and 1-pentyne from Aldrich. Unless otherwise stated, com-

mercially purchased materials were used without further purification. Deuteriochloroform was predried with calcium hydride and vacuum transferred and stored over 4 Å molecular sieves. The ruthenium complexes $[(p\text{-cymene})RuCl_2]_2$[44] and [(*p*-cymene)Ru(MeO-BIPHEP)Cl][SbF_6][23b] were prepared as previously described. ^1H and $^{31}P\{^1H\}$ and $^{13}C\{^1H\}$ NMR spectra were recorded on a JEOL LAMBDA 500 or Bruker AC 200, AMX 300, and DRX 500 machines. Purification of reaction products was carried out by column chromatography on reagent silica gel (60−200 mesh).

Synthesis of [(*p*-cymene)Ru(1,2,3,4-Me$_4$-NUPHOS)Cl][SbF$_6$] (2a). A solution of 1,2,3,4-Me$_4$-NUPHOS (0.200 g, 0.42 mmol) and $NaSbF_6$ (0.108 g 0.42 mol) in dichloromethane was added to $[(p\text{-cymene})RuCl_2]_2$ (0.12 g, 0.2 mmol), and the resulting mixture was stirred at room temperature for 12 h, after which time it was filtered through Celite and the solvent removed to give **2a** as a spectroscopically pure yellow-orange powder in quantitative yield. Crystallization by slow diffusion of a concentrated dichloromethane solution layered with hexane gave **2a** as orange crystals in 86% yield (0.35 g). Although we were unable to grow crystals of the hexafluoroantimonate salt of **2a** suitable for analysis by single-crystal X-ray crystallography, crystals of the corresponding perchlorate salt, prepared by replacement of $NaSbF_6$ with $NaClO_4$ in the above procedure, were obtained by slow diffusion of hexane into a concentrated dichloromethane solution at room temperature. $^{31}P\{^1H\}$ NMR (121.4 MHz, $CDCl_3$, δ): 39.8 (d, $^2J_{PP}$ = 60.5 Hz, P_A), 27.9 (d, $^2J_{PP}$ = 60.5 Hz, P_B). ^1H NMR (500.1 MHz, $CDCl_3$, δ): 7.8−6.9 (m, 20H, C_6H_5), 6.05 (d, J_{HH} = 6.0 Hz, 1H, *p*-cymene), 5.94 (d, J_{HH} = 7.0 Hz, 1H, *p*-cymene), 4.38 (br d, J_{HH} = 7.0 Hz, 1H, *p*-cymene), 4.26 (d, J_{HH} = 7.0 Hz, 1H, p-cymene), 3.05 (sept, J_{HH} = 6.9 Hz, 1H, C*H*Me$_2$), 1.91 (s, 3H, *p*-cymene-CH_3), 1.79 (d, J_{PH} = 11.6 Hz, 3H, CH_3), 1.43 (d, J_{PH} = 10.5 Hz, 3H, CH_3), 1.37 (d, J_{HH} = 6.9 Hz, 3H, CH(CH_3)$_2$), 1.32 (s, 3H, CH_3), 0.97 (d, J_{HH} = 6.9 Hz, 3H, CH(CH_3)$_2$), 0.93 (s, 3H, CH_3). MS (FAB$^+$): calcd M^+ 749; found 749 $[M]^+$, 714 $[M - Cl]^+$, 615 $[M - p\text{-cymene}]^+$. Anal. Calcd for $C_{42}H_{46}ClF_6P_2RuSb$ C, 51.21; H, 4.71. Found: C, 51.63; H, 5.01.

Synthesis of [(*p*-cymene)Ru(1,4-Et$_2$-2,3-*cyclo*-C$_6$H$_8$-NUPHOS)Cl][SbF$_6$] (2b). Compound **2b** was prepared according to the procedure described above for **2a** and was isolated as orange-yellow crystals in 60% yield by slow diffusion of hexane into a chloroform solution at room temperature. $^{31}P\{^1H\}$ NMR (121.4 MHz, $CDCl_3$, δ): 37.9 (d, $^2J_{PP}$ = 66.0 Hz, P_A), 22.0 (d, $^2J_{PP}$ = 66.0 Hz, P_B). ^1H NMR (500.1 MHz, $CDCl_3$, δ): 7.87−7.15 (m, 20H, C_6H_5), 6.15 (d, J_{HH} = 6.8 Hz, 1H, *p*-cymene), 5.68 (d, J_{HH} = 6.1 Hz, 1H, *p*-cymene), 5.36 (br d, J_{HH} = 6.1 Hz, 1H, *p*-cymene), 4.63 (d, J_{HH} = 6.8 Hz, 1H, *p*-cymene), 3.10 (sept, J_{HH} = 6.8 Hz, 1H, C*H*Me$_2$), 2.56 (m, 2H, CH_2CH$_3$), 2.30 (m, 2H, CH_2CH$_3$), 2.24 (m, 1H, Cy-*H*), 1.82 (s, 3H, *p*-cymene-CH_3), 1.6−1.4 (m, 6H, Cy-*H*), 1.41 (d, J_{HH} = 6.8 Hz, 3H, CH(CH_3)$_2$), 1.1 (br m, 1H, Cy-*H*), 0.96 (d, J_{HH} = 6.8 Hz, 3H, CH(CH_3)$_2$), 0.38 (t, J_{HH} = 7.4 Hz, CH$_2$CH_3), 0.24 (t, J_{HH} = 7.4 Hz, CH$_2$CH_3). MS (FAB$^+$): calcd M^+ 803; found 803 $[M]^+$, 768 $[M - Cl]^+$, 669 $[M - p\text{-cymene}]^+$. Anal. Calcd for $C_{46}H_{52}ClF_6P_2RuSb.2CHCl_3$ C, 45.11; H, 4.26. Found: C, 45.47; H, 4.41.

Synthesis of [(*p*-cymene)Ru(*P*,*P*,η^2(*C*)-1,2,3,4-Me$_4$-NUPHOS)][SbF$_6$]$_2$ (3a). A solution of **2a** (0.100 g, 0.1 mmol) in dichloromethane (4 mL) was treated with $AgSbF_6$ (0.034 g, 0.1 mmol) and stirred for 30 min at room temperature. The resulting mixture was filtered through Celite and the solvent removed under reduced pressure to afford **3a** as a spectroscopically pure yellow powder, which was crystallized by slow diffusion of toluene into a dichloromethane solution at room temperature (0.09 g 76%). $^{31}P\{^1H\}$ NMR (121.4 MHz, $CDCl_3$, δ): 78.9 (d, $^2J_{PP}$ = 38.7 Hz, P_A), 6.5 (d, $^2J_{PP}$ = 38.7 Hz, P_B). ^1H NMR (500.1 MHz, $CDCl_3$, δ): 8.09−6.96 (m, 20H, C_6H_5), 6.91 (d, J_{HH} = 6.5 Hz, 1H, *p*-cymene), 6.61 (d, J_{HH} = 6.0 Hz, 1H, *p*-cymene), 6.35 (d, J_{HH} = 6.0 Hz, 1H, *p*-cymene), 5.82 (d, J_{HH} = 6.5 Hz, 1H, *p*-cymene), 2.79 (d, J_{PH} = 9.8 Hz, 3H, CH_3), 2.72 (m, 1H, C*H*Me$_2$), 2.35 (br s, 6H, 2 × CH_3), 2.0 (br s, 3H, *p*-cymene CH_3), 1.1 (d, J_{HH} = 6.8 Hz, 3H, CH*Me*$_2$), 0.89 (d, J_{PH} = 11.3 Hz, 3H, CH_3), 0.59 (d, J_{HH} = 6.8 Hz, 3H, CH*Me*$_2$). ^{13}C NMR (125.13 MHz, $(CD_3)_2C{=}O$, δ): 161.4 (d, J_{PC} = 28.0 Hz, *C*Me), 140.8−122.5 (m, C_6H_5 + *p*-cymene), 108.0 (s, C_6H_4), 106.1 (s, C_6H_4), 105.7 (d, J_{PC} = 7.1, 5.0 Hz, η^2-C=C), 103.9 (s, C_6H_4), 103.6 (s, C_6H_4), 65.1 (d, J_{PC} = 30 Hz, η^2-C=C), 33.8 (s, *C*HMe$_2$), 27.3 (d, J_{PC} = 8.0 Hz, C*Me*), 26.7 (s, C*Me*), 24.8 (s, CH*Me*$_2$), 23.9 (d, J_{PC} = 7.1 Hz, C*Me*), 22.8 (s, CH*Me*$_2$), 21.6 (s, *p*-cymene Me), 17.3 (s, C*Me*). MS (FAB$^+$): calcd M^{2+} 714; found 950 $[M + SbF_6]^+$. Anal. Calcd for $C_{42}H_{46}F_{12}P_2RuSb_2$ C, 42.56; H, 3.91. Found: C, 42.87; H, 4.11.

Synthesis of [(*p*-cymene)Ru(*P*,*P*,η^2(*C*)-1,4-Et$_2$-2,3-*cyclo*-C$_6$H$_8$-NUPHOS)][SbF$_6$]$_2$ (3b). Compound **3b** was prepared according to the procedure described above for **3a** and was isolated as yellow crystals in 60% yield by slow diffusion of hexane into a dichloromethane solution at room temperature. $^{31}P\{^1H\}$ NMR (121.4 MHz, $CDCl_3$, δ): 82.1 (d, $^2J_{PP}$ = 38.7 Hz, P_A), 9.0 (d, $^2J_{PP}$ = 38.7 Hz, P_B). ^1H NMR (500.1 MHz, $CDCl_3$, δ): 7.89−7.24 (m, 16H, C_6H_5), 6.90 (br s, 2H, C_6H_5), 6.81 (br s, 2H, C_6H_5), 6.34 (d, J_{HH} = 6.6 Hz, 1H, *p*-cymene C*H*), 6.31 (d, J_{HH} = 6.6 Hz, 1H, *p*-cymene C*H*), 5.65 (d, J_{HH} = 6.6 Hz, 2H, *p*-cymene C*H*), 3.06 (m, 1H, Cy-*H*), 2.87 (m, 1H, Cy-*H*), 2.73 (d br, J_{HH} = 10.1 Hz, 1H, Cy-*H*), 2.51 (d br, J_{HH} = 10.1 Hz, 1H, Cy-*H*), 2.27 (m, 1H, Cy-H), 2.26 (sept, J_{HH} = 6.6 Hz, 1H, C*H*Me$_2$), 2.21 (br d, J_{HH} = 10.1 Hz, 1H, Cy-*H*), 2.04 (m, 1H, Cy-*H*), 1.78 (s, 3H, *p*-cymene CH_3), 1.77 (m, 1H, Cy-*H*), 1.18−1.0 (m, 2H, CH_2CH$_3$), 0.76 (t, J_{HH} = 7.6 Hz, 3H, CH_3), 0.43 (t, J_{HH} = 7.6 Hz, 3H, CH$_2$CH_3). ^{13}C NMR (125.13 MHz, CD_2Cl_2, δ): 136.1−125.4 (m, C_6H_5 + *p*-cymene + C=C), 117.4 (s, *p*-cymene), 105.8 (s, *p*-cymene), 102.1 (dd, J_{PC} = 6.1, 4.0 Hz, η^2-*C*=C), 101.8 (s, *p*-cymene), 99.3 (s, *p*-cymene), 96.7 (s, *p*-cymene), 62.6 (d, J_{PC} = 26 Hz, η^2-C=*C*), 30.8 (s, Cy-*C*H$_2$), 30.1 (s, *p*-cymene-*C*HMe$_2$), 27.6 (s, *p*-cymene-C*Me*), 29.6 (s, Cy-*C*H$_2$), 27.3 (s, Cy-*C*H$_2$), 25.4 (Cy-*C*H$_2$), 22.2 (s, *p*-cymene-CH*Me*$_2$), 21.9 (s, *C*H$_2$CH$_3$), 20.9 (d, J_{PC} = 4.9 Hz, *C*H$_2$CH$_3$), 19.7 (s, *p*-cymene-CH*Me*$_2$), 13.1 (s, CH$_2$*C*H$_3$), 12.5 (s, CH$_2$*C*H$_3$). MS (FAB$^+$): calcd M^{2+} 768; found 1003 $[M + SbF_6]^+$. Anal. Calcd for $C_{46}H_{52}F_{12}P_2RuSb_2$ C, 44.58; H, 4.23. Found: C, 44.91; H, 4.57.

Synthesis of [(*p*-cymene)Ru(BIPHEP)Cl][SbF$_6$] (4a). Compound **4a** was prepared according to the procedure described above for **2a** and was isolated as deep orange crystals in 78% yield by slow diffusion of hexane into a chloroform solution at room temperature. X-ray quality crystals were grown by diffusion of hexane into a concentrated dichloromethane solution. $^{31}P\{^1H\}$ NMR (121.4 MHz, $CDCl_3$, δ): 40.8 (d, J_{PP} = 63.0 Hz, PPh_2), 29.1 (d, J_{PP} = 63.0 Hz, PPh_2). ^1H NMR (500.1 MHz, $CDCl_3$, δ): 7.87−7.14 (m, 26H, C_6H_5 + biphenyl), 6.66 (dd, J = 7.2, 1.7 Hz, 1H, biphenyl), 6.27 (dd, J = 7.0, 1.6 Hz, 1H, biphenyl), 5.83 (d, J_{HH} = 6.7 Hz, 1H, *p*-cymene-C*H*), 5.36 (d, J_{HH} = 6.1 Hz, 4H, *p*-cymene-C*H*), 4.48 (d, J_{HH} = 6.1 Hz, 1H, *p*-cymene-C*H*), 4.42 (d, J_{HH} = 6.1 Hz, 4H, *p*-cymene-C*H*), 2.99 (sept, J_{HH} = 6.8 Hz, 2H, C*H*Me$_2$), 1.83 (s, 3H, *p*-cymene-CH_3), 1.29 (d, J_{HH} = 6.8 Hz, 3H, *p*-cymene-CH*Me*$_2$), 0.96 (d, J_{HH} = 6.8 Hz, 3H, *p*-cymene-CH*Me*$_2$). ^{13}C NMR (125.13 MHz, $CDCl_3$, δ): 146−122 (m, C_6H_5 + biphenyl), 114.2 (s, *p*-cymene), 108.6 (s, *p*-cymene), 103.2 (s, *p*-cymene), 101.6 (s, *p*-cymene), 96.9 (s, *p*-cymene-*C*H), 85.9 (s, *p*-cymene-*C*H), 29.5 (s, *p*-cymene-*C*HMe$_2$), 21.7 (s, *p*-cymene-CH*Me*$_2$), 20.6 (s, *p*-cymene-CH*Me*$_2$), 18.2 (s, *p*-cymene-*C*H$_3$). Anal. Calcd for $C_{46}H_{42}ClF_6P_2RuSb{\cdot}2CH_2Cl_2$, 48.09; H, 3.87. Found: C, 48.39; H, 4.13.

Attempted Preparation of [(*p*-cymene)Ru(BIPHEP)][SbF$_6$]$_2$ (5a) and [(*p*-cymene)Ru(MeO-BIPHEP)][SbF$_6$]$_2$ (5b). Initially, a solution of **4a** (0.100 g, 0.097 mmol) in dichloromethane (4 mL) was treated with $AgSbF_6$ (0.033 g, 0.097 mmol) and stirred for 1 h at room temperature, after

(44) Bennett, M. A.; Huang, T.-N.; Matheson, T. W.; Smith, A. K. *Inorg. Synth.* **1981**, *21*, 74.

which time there was no sign of reaction, as evidenced by ^{31}P NMR spectroscopy. The solution was subsequently refluxed for 24 h, then filtered through Celite. The solvent was removed and the ^{31}P NMR spectrum of the this crude product recorded, which contained two distinct sets of resonances, a major pair of doublets associated with **4a** and a minor set of broad resonances at δ 65.1 and 5.0 corresponding to approximately 20% of the desired product. A similar level of conversion was obtained during the reaction of **4b** with $AgSbF_6$ under similar conditions, as evidenced by characteristic ^{31}P resonances at δ 67.1 and 7.7.

Synthesis of [{(*p*-cymene)RuCl}$_2$(*μ*-dppb)] (6). A solution of dppb (0.200 g, 0.47 mmol) and [(*p*-cymene)$RuCl_2$]$_2$ (0.280 g, 0.46 mmol) in dichloromethane (20 mL) was stirred for 4 h, after which time the reaction mixture was filtered and the solvent removed to give **6** as a spectroscopically pure orange-red solid in 98% yield (0.465 g). Crystals suitable for single-crystal X-ray structure determination were grown by slow diffusion of hexane into a dichloromethane solution at room temperature. $^{31}P\{^1H\}$ NMR (121.4 MHz, $CDCl_3$, δ): 24.9 (s, PPh_2). ^1H NMR (500.1 MHz, $CDCl_3$, δ): 7.6 (dt, J = 9.6, 1.2 Hz, 8H, C_6H_5), 7.38 (m, 12H, C_6H_5), 5.11 (d, J_{HH} = 6.0 Hz, 4H, *p*-cymene-C*H*), 4.94 (d, J_{HH} = 6.0 Hz, 4H, *p*-cymene-C*H*), 2.26 (sept, J_{HH} = 6.9 Hz, 2H, C*H*Me_2), 2.11 (br, 4H, dppb-CH_2), 1.71 (s, 6H, *p*-cymene-CH_3), 0.8 (br, 4H, dppb-CH_2), 0.67 (d, J_{HH} = 6.9 Hz, 12H, *p*-cymene-CH*Me*$_2$). ^{13}C NMR (125.13 MHz, $CDCl_3$, δ): 132.4 (s, C_6H_5), 131.6 (d, J_{PC} = 42 Hz, C_6H_5), 129.7 (s, C_6H_5), 127.4 (s, C_6H_5), 106.5 (s, *p*-cymene), 92.8 (s, *p*-cymene), 89.6 (d, J_{PC} = 4.0 Hz, *p*-cymene-*C*H), 84.8 (d, J_{PC} = 5.7 Hz, *p*-cymene-*C*H), 29.2 (s, *p*-cymene-*C*HMe_2), 23.9 (d, J_{PC} = 12.1 Hz, PCH_2CH_2), 21.8 (d, J_{PC} = 28.0 Hz, P*C*H_2), 20.2 (s, *p*-cymene-CH*Me*$_2$), 16.2 (s, *p*-cymene-*C*H_3). Anal. Calcd for $C_{52}H_{56}Cl_4P_2Ru_2$ C, 55.50; H, 5.43. Found: C, 55.89; H, 5.55.

Attempted Preparation of [(*p*-cymene)Ru(1,2,3,4-Me$_4$-NUPHOS)(py)][SbF$_6$]$_2$. A dichloromethane solution of **3a** (0.08 g, 0.067 mmol) and pyridine (6.4 μl, 0.08 mmol) was stirred for 30 min, during which time the color changed from pale yellow to brown-yellow. The reaction mixture was filtered, the solvent removed, and the residue crystallized by slow diffusion of hexane into a concentrated dichloromethane solution at room temperature to afford **7** as a yellow crystalline solid in 87% yield (0.057 g). $^{31}P\{^1H\}$ NMR (121.4 MHz, $CDCl_3$, δ): 73.3 (s, PPh_2), 68.4 (s, PPh_2). ^1H NMR (500.1 MHz, $CDCl_3$, δ): 8.10 (t, J = 7.5 Hz, 2H, C_6H_5), 7.8 (dd, J = 11.0 Hz, 7.5 Hz, 2H, C_6H_5), 7.7−7.4 (m, 10H, C_6H_5), 7.30 (t, J = 7.6 Hz, 2H, C_6H_5), 7.17 (dt, J = 7.7, 3.0 Hz, 2H, C_6H_5), 6.98 (dd, J = 11.0, 7.5 Hz, 2H, C_6H_5), 6.16 (d, J_{HH} = 9.5 Hz, 1H, *p*-cymene), 5.74 (d, J_{HH} = 9.5 Hz, 1H, *p*-cymene), 5.64 (d, J_{HH} = 9.5 Hz, 1H, *p*-cymene), 5.01 (dq, J_{PH} = 17.8 Hz, $J_{H}H$ 12.5 Hz, Ph_2P-(O)C*H*Me), 4.70 (d, J_{HH} = 9.5 Hz, 1H, *p*-cymene), 2.23 (s, 3H, *p*-cymene-CH_3), 1.49 (dd, J_{PH} = 17.8 Hz, J_{HH} = 12.5 Hz, 1H, Ph_2P(O)CH*Me*), 1.45 (d, J_{PH} = 9.1 Hz, 3H, C*Me*), 1.42 (sept, J_{HH} = 7.0 Hz, 1H, *p*-cymene-CH*Me*$_2$), 1.16 (s, 3H, CMe), 0.98 (d, J_{HH} = 7.0 Hz, 3H, CH*Me*$_2$), 0.78 (d, J_{HH} = 7.0 Hz, 3H, CH*Me*$_2$), 0.74 (s, 3H, C*Me*). Anal. Calcd for $C_{42}H_{47}F_6OP_2RuSb$ C, 52.19; H, 4.90. Found: C, 52.58; H, 5.13.

General Procedure for Ruthenium-Catalyzed Addition of Benzoic Acid to 1-Octyne. Method A. In a typical procedure a solution of **2a** (0.0423 g, 0.043 mmol) in 1,2-dichloroethane (1 mL) was treated with $AgSbF_6$ (0.0147 g, 0.043 mmol) and stirred for 0.5 h, after which time benzoic acid (0.106 g, 0.87 mmol) and 1-octyne (0.130 mL, 0.88 mmol) were added. The resulting reaction mixture was stirred for 24 h at 60 °C, then cooled to room temperature, diluted with dichloromethane (20 mL), washed with $NaHCO_3$, and dried over $MgSO_4$. The crude residue was purified by column chromatography over silica gel (60−200 mesh, 5% ethyl acetate in hexane). The *E*/*Z* ratio and the regioselectivity were determined by ^1H NMR spectroscopy.[44]

General Procedure for Ruthenium-Catalyzed Addition of Benzoic Acid to 1-Octyne. Method B. In a typical procedure a solution of **2a** (0.0423 g, 0.043 mmol) and 1-octyne (0.130 mL, 0.88 mmol) in 1,2-dichloroethane (1 mL) was stirred for 24 h at 60 °C, then cooled to room temperature, diluted with dichloromethane (20 mL), washed with $NaHCO_3$, and dried over $MgSO_4$. The crude residue was purified by column chromatography over silica gel (60−200 mesh, 5% ethyl acetate in hexane).

General Procedure for Ruthenium-Catalyzed Addition of Benzoic Acid to 1-Pentyne. The catalytic hydrocarboxylation of 1-pentyne was performed according to methods A and B described above for 1-ocytne in dichloromethane for 96 h at 35 °C. The crude residue was purified by column chromatography over silica gel (60−200 mesh, 5% ethyl acetate in hexane).

General Procedure for Ruthenium-Catalyzed Addition of Benzoic Acid to Phenylacetylene. The catalytic hydrocarboxylation of phenylaceylene was performed according to methods A and B described above for 1-ocytne in 1,2-dichloroethane for 20 h at 60 °C. The crude residue was purified by column chromatography over silica gel (60−200 mesh, 5% ethyl acetate in hexane).

Crystal Structure Determinations. Crystals of **2a**, **2b**, **3a**, **4a**, **6**, and **7** were examined with Mo Kα radiation (λ = 0.71073 Å) on Bruker SMART and Bruker-Nonius KappaCCD diffractometers at 150 K. Selected crystal data are given in Table 5, and further details of the structure determination are in the Supporting Information. Semiempirical absorption corrections were applied, based on repeated and symmetry-equivalent reflections.[46] The structures were solved by direct methods and refined by least-squares methods on all unique F^2 values, with anisotropic displacement parameters, and with constrained riding hydrogen atoms; U(H) was set at 1.2 (1.5 for methyl groups) times U_{eq} of the parent atom. Disorder over two distinct positions was resolved and refined for the anion and one ^{i}Pr group of **2a**, the anions of **2b** and **3a**, and the dichloromethane solvent molecule of **4a**. More extensive disorder could not be modeled for solvent molecules in most of the structures, and these were treated with the SQUEEZE procedure of PLATON.[47] **2a** was found to be an inversion twin, with 23(3)% of the second component, and **4a** was a nonmerohedral twin, with approximately 2:1 ratio of the two components; merging of symmetry-equivalent reflections is not possible before refinement in this case. The largest features in final difference syntheses are close to heavy atoms and disordered groups. Programs were Bruker AXS SMART and SAINT, Nonius COLLECT and EvalCCD, and SHELXTL.[48]

Acknowledgment. We gratefully acknowledge the EPSRC (R.K.R.), the University of Newcastle upon Tyne and the McClay Trust (C.R.N.) for funding and Johnson Matthey for generous loans of palladium salts.

Supporting Information Available: For **2a**, **2b**, **3a**, **4a**, **6**, and **7** details of structure determination, atomic coordinates, bond lengths and angles, and displacement parameters in CIF format. This material is available free of charge via the Internet at http://pubs.acs.org. Observed and calculated structure factor tables are available from the authors upon request.

OM050014J

(45) Rotem, M.; Shvo, Y. *J. Organomet. Chem.* **1993**, *448*, 189.
(46) Sheldrick, G. M. *SADABS*; University of Göttingen: Germany, 1997.
(47) Spek, A. L. *J. Appl. Crystallogr.* **2003**, *36*, 7.
(48) (a) *SMART* and *SAINT* software for CCD diffractometers; Bruker AXS Inc.: Madison, WI, 2001. (b) *COLLECT* software for KappaCCD; Nonius BV: Delft, The Netherlands, 1998. (c) Duisenberg, A. J. M.; Kroon-Batenburg, L. M. J.; Schreurs, A. M. M. *J. Appl. Crystallogr.* **2003**, *36*, 220. (d) Sheldrick, G. M. *SHELXTL user manual*, version 6; Bruker AXS, Inc.; Madison, WI, 2001.